



# A Subset of Nucleus Accumbens Neurons Receiving Dense and Functional Prelimbic Cortical Input Are Required for Cocaine Seeking

## OPEN ACCESS

### Edited by:

M. Foster Olive,  
Arizona State University, United States

### Reviewed by:

Yonatan M. Kupchik,  
Hebrew University of Jerusalem, Israel  
Alban de Kerchove d'Exaerde,  
Université Libre de Bruxelles (ULB),  
Belgium

### \*Correspondence:

Michael D. Scofield  
Scofield@musc.edu

### † Present address:

Benjamin M. Siemsen,  
Department of Anatomy and  
Neurobiology, University of Maryland  
School of Medicine, Baltimore, MD,  
United States

‡ These authors have contributed  
equally to this work

### Specialty section:

This article was submitted to  
Cellular Neuropathology,  
a section of the journal  
Frontiers in Cellular Neuroscience

Received: 27 December 2021

Accepted: 02 February 2022

Published: 24 February 2022

### Citation:

Siemsen BM, Barry SM,  
Vollmer KM, Green LM, Brock AG,  
Westphal AM, King RA, DeVries DM,  
Otis JM, Cowan CW and Scofield MD  
(2022) A Subset of Nucleus  
Accumbens Neurons Receiving  
Dense and Functional Prelimbic  
Cortical Input Are Required  
for Cocaine Seeking.  
Front. Cell. Neurosci. 16:844243.  
doi: 10.3389/fncel.2022.844243

Benjamin M. Siemsen<sup>1†‡</sup>, Sarah M. Barry<sup>2†</sup>, Kelsey M. Vollmer<sup>2</sup>, Lisa M. Green<sup>2</sup>,  
Ashley G. Brock<sup>1</sup>, Annaka M. Westphal<sup>1</sup>, Raven A. King<sup>1</sup>, Derek M. DeVries<sup>2</sup>,  
James M. Otis<sup>2</sup>, Christopher W. Cowan<sup>2</sup> and Michael D. Scofield<sup>1,2\*</sup>

<sup>1</sup> Department of Anesthesia and Perioperative Medicine, Medical University of South Carolina, Charleston, SC, United States, <sup>2</sup> Department of Neuroscience, Medical University of South Carolina, Charleston, SC, United States

**Background:** Prelimbic cortical projections to the nucleus accumbens core are critical for cue-induced cocaine seeking, but the identity of the accumbens neuron(s) targeted by this projection, and the transient neuroadaptations contributing to relapse within these cells, remain unknown.

**Methods:** Male Sprague-Dawley rats underwent cocaine or sucrose self-administration, extinction, and cue-induced reinstatement. Pathway-specific chemogenetics, patch-clamp electrophysiology, *in vivo* electrochemistry, and high-resolution confocal microscopy were used to identify and characterize a small population of nucleus accumbens core neurons that receive dense prefrontal cortical input to determine their role in regulating cue-induced cocaine and natural reward seeking.

**Results:** Chemogenetic inhibition of prefrontal cortical projections to the nucleus accumbens core suppressed cue-induced cocaine relapse and normalized real-time cue-evoked increases in accumbens glutamate release to that of sucrose seeking animals. Furthermore, chemogenetic inhibition of the population of nucleus accumbens core neurons receiving the densest prefrontal cortical input suppressed cocaine, but not sucrose seeking. These neurons also underwent morphological plasticity during the peak of cocaine seeking in the form of dendritic spine expansion and increased ensheathment by astroglial processes at large spines.

**Conclusion:** We identified and characterized a unique subpopulation of nucleus accumbens neurons that receive dense prefrontal cortical input. The functional specificity of this subpopulation is underscored by their ability to mediate cue-induced cocaine relapse, but not sucrose seeking. This subset of cells represents a novel target for addiction therapeutics revealed by anterograde targeting to interrogate functional circuits imbedded within a known network.

**Keywords:** cocaine, prefrontal, nucleus accumbens, sucrose, glutamate, astrocytes

## INTRODUCTION

Relapse to cocaine use can be precipitated by cues or contexts predicting cocaine (Kosten et al., 2006) which activate key cortical and limbic regions involved in craving (Childress et al., 1999). Pre-clinical models of cue-induced cocaine craving rely upon the use of self-administration (SA), abstinence (with or without extinction training), and re-exposure to cocaine-paired cues or contexts, which is crucial for interrogating neuronal circuits and cell types mediating cocaine relapse (Farrell et al., 2018).

Cue-mediated activation of prelimbic (PrL) cortical glutamatergic neurons, particularly their projection to the nucleus accumbens core (NAcore), is required for reinstatement of cocaine seeking after extinction (Kalivas et al., 2005; McGlinchey et al., 2016). Within the NAcore, the homeostatic regulation of glutamate is disrupted following extinction of cocaine self-administration (Kalivas, 2009) due to dysfunction in astrocyte-mediated glutamate clearance (Scofield et al., 2016a), among other adaptations (Moran et al., 2005; Scofield et al., 2016b; Testen et al., 2018). Together, cocaine-induced alterations in neural function yield enhanced glutamate release in the NAcore when animals are exposed to cocaine cues, driving drug seeking (Smith et al., 2017; Siemsen et al., 2020). Accordingly, pharmacological inhibition of the PrL cortex (McLaughlin and See, 2003) or optogenetic inhibition of PrL terminals in the NAcore (Stefanik et al., 2013, 2016) suppresses cue-induced cocaine seeking, without affecting seeking for natural rewards (Caballero et al., 2019). Downstream from the PrL cortex, NAcore MSNs integrate inputs from multiple regions to guide motivated behavior (Girault, 2012). PrL inputs represent a major driver of NAcore neurons (Finch, 1996) and neural processes within the NAcore that guide motivated behavior are known to be disrupted by cocaine (see Carelli, 2002; Kalivas, 2008; Kalivas and O'Brien, 2008 for reviews). While electrical stimulation of the PFC evokes excitatory post-synaptic potentials (EPSPs) in the vast majority of NAcore neurons, action potential firing is observed in less than half of NAcore neurons (O'Donnell and Grace, 1995; Finch, 1996). Additionally, when relatively weak PFC stimulation is employed, ~20% of NAcore neurons exhibit spike firing, suggesting that a subpopulation of NAcore neurons receives the majority of PrL inputs (Finch, 1996) and that there is heterogeneity of functional innervation of NAcore MSNs by PrL neurons. Given the importance of PrL afferents in driving cocaine seeking, the NAcore neurons receiving the majority of PrL inputs are a particularly relevant population for understanding relapse vulnerability.

Cue-induced reinstatement of several classes of drugs, including cocaine, elicits a transient increase in synaptic strength in NAcore medium spiny neurons (MSNs) (Shen et al., 2011; Gipson et al., 2013a,b). During the peak of cocaine seeking, NAcore MSNs undergo PrL-dependent morphological and synaptic plasticity (enhanced dendritic spine head diameter and AMPA/NMDA ratio) – events that are required for cue-induced cocaine seeking (Gipson et al., 2013a). Moreover, following cocaine or heroin SA, Scofield et al. (2016b), Kruyer et al. (2019), and Siemsen et al. (2019) astrocyte processes exhibit

reduced contact with bulk NAcore synapses (i.e., Synapsin-I<sup>+</sup> synapses), which contributes to heightened cue-induced glutamatergic signaling. During cued heroin seeking, astrocyte processes “re-associate” with NAcore synapses, presumably to limit cue-induced glutamate signaling, dampening heroin seeking (Kruyer et al., 2019). However, the specific MSN population whereby increased astrocyte association occurs, whether this occurs on functionally relevant synapses, and whether this holds true for cue-induced cocaine seeking, is unknown. This is important given that astrocyte regulation of synaptic transmission is highly specific and that astrocytic processes can interact and regulate both excitatory and inhibitory synapses in response to changes in overall network activity (Dallerac et al., 2018; Durkee and Araque, 2019; Gordleeva et al., 2019).

In this study, we systematically evaluated the contribution of PrL neurons projecting to the NAcore (PrL<sup>NAcore</sup>) in cue-induced cocaine and sucrose seeking using an intersectional chemogenetic viral vector approach, while simultaneously measuring glutamate release in the NAcore during seeking. We then identified a novel sub-population of NAcore neurons that receive the most dense and active PrL cortical innervation (NAcore<sup>PrL</sup>) using an anterograde, transsynaptic AAV1-Cre vector in the PrL and Cre-dependent constructs in the NAcore. We used this combinatorial viral vector approach to examine (a) the role of NAcore<sup>PrL</sup> neurons in cocaine and sucrose seeking and (b) the regulation of NAcore<sup>PrL</sup> synapses and their ensheathing astrocytic processes in cue-induced cocaine seeking.

## MATERIALS AND METHODS

### Animal Subjects and Surgery

Male Sprague-Dawley rats ( $N = 82$ ) were used for all experiments. All animal use protocols were approved by the Medical University of South Carolina and were performed according to the National Institutes of Health Guide for the Care and Use of Laboratory Animals (8th ed., 2011). Viral vector information can be found in **Table 1**. Detailed methods can be found in the **Supplementary Information**.

### Drugs

Cocaine hydrochloride (NIDA, Research Triangle Park NC; 200  $\mu\text{g}/50 \mu\text{l}$  bolus) was dissolved in sterile saline for SA experiments. Clozapine-*N*-Oxide (CNO) was obtained through the National Institute of Mental Health Chemical Synthesis Program. CNO was dissolved in 5% DMSO in sterile saline and was administered at a dose of 5 mg/kg (i.p.) 30 min before testing.

### Cocaine and Sucrose Self-Administration

Cocaine and sucrose SA (SA) were performed as previously described (Giannotti et al., 2018; Siemsen et al., 2018a,b, 2020). Briefly, rats were mildly food-deprived (~15 g rat chow/day) to increase exploration prior to beginning SA and were then maintained at 20 g/day for the remainder of the experiment.

**TABLE 1** | Virus, source, titer, injection location, and purpose for all viral vectors used.

Virus	Source	Titer (vg/ml)	Injection site	Purpose
AAV1-CamKII $\alpha$ -Cre-0.4-SV40	Addgene	1.2- $1.9 \times 10^{13}$	PrL	Transsynaptic Cre expression
AAV5-GfaABC1D-Lck-GFP	University of North Carolina Vector Core	$0.55 \times 10^{13}$	NAcore	GFP expression in astrocyte membrane processes
AAV2-hSyn-DIO-hM4Di	Addgene	$2.5 \times 10^{13}$	PrL; NAcore	Cre-dependent hM4Di expression
AAV2-hSyn-DIO-mCherry	Addgene	$1.6 \times 10^{13}$	PrL; NAcore	Cre-dependent mCherry expression
AAV1-CAG-Flex-Ruby2sm-Flag-WPRE-SV40	Addgene	$1.1 \times 10^{13}$	NAcore	Cre-dependent expression of Flag-tagged smFP
AAV2-EF1a-DIO-hChR2(H134R)-EYFP	University of North Carolina Vector Core	$1.6 \times 10^{12}$	PrL	Cre-dependent Channel Rhodopsin expression
AAVrg-hSyn-Cre-WPRE-hGH	Addgene	$2.1 \times 10^{13}$	NAcore	Expression of Cre in neurons projecting to NAcore

Rats were weighed daily, and catheters were flushed with sterile saline prior to daily SA sessions. Rats then underwent SA [Fixed ratio (FR) 1 schedule of reinforcement] in standard MedPC operant chambers (Med Associates, St. Albans, VT, United States) fixed with two retractable levers, a house light, tone generator, sucrose pellet dispenser, and two lights above each lever for 2 h/day (12–14 days). Presses on the active lever elicited a light and tone cue-complex followed by a single infusion of cocaine or a single 45 mg flavored sucrose pellet (Bioserv, Flemington, NJ #F0025, United States) followed by a 20 s timeout period. Presses on the inactive lever had no programmed consequence. The day after the final SA session, rats either entered extinction training or received an intra-NAcore cannula implantation for electrochemical experiments. Active lever presses (ALP), inactive lever presses (ILP) and infusions earned are shown within each figure for all SA experiments.

## Extinction and Cue-Induced Reinstatement

During daily extinction sessions (2 h/day) ALPs had no programmed consequence. Animals underwent extinction sessions until they met criterion (average  $\leq 25$  ALPs over the last 2 days). Rats then underwent a cue-induced reinstatement test whereby ALPs elicited the light and tone cue-complex, but no cocaine or sucrose delivery. Yoked saline animals were sacrificed 24 h after the final extinction session without undergoing reinstatement. At the beginning of each reinstatement session, a single non-contingent cue was presented. Following the 2-h reinstatement session, a subset of rats were perfused 15 min after the session for Fos immunohistochemistry (see below). Virus expression in both the PrL cortex and NAcore were mapped according to the atlas of Paxinos and Watson.

## Perfusions and Immunohistochemistry

Antisera information can be found in the key resource table. Detailed methods can be found in the **Supplementary Information**.

## Patch-Clamp Electrophysiology

Rats were anesthetized with isoflurane and rapidly decapitated for brain extraction. Brains were sectioned (300  $\mu$ m) using a vibratome (Leica VT 1200) in ice-cold, oxygenated sucrose cutting solution containing (in mM): 225 sucrose, 119 NaCl, 1.0 NaH<sub>2</sub>PO<sub>4</sub>, 4.9 MgCl<sub>2</sub>, 0.1 CaCl<sub>2</sub>, 26.2 NaHCO<sub>3</sub>, 1.25 glucose,  $\sim 305$  mOsm. Brain slices recovered for 30 min in warm (32°C) aCSF containing (in mM): 119 NaCl, 2.5 KCl, 1.0 NaH<sub>2</sub>PO<sub>4</sub>, 1.3 MgCl<sub>2</sub>, 2.5 CaCl<sub>2</sub>, 26.2 NaHCO<sub>3</sub>, 15 glucose,  $\sim 305$  mOsm. During recording, slices were perfused with room-temperature aCSF (1 mL/min). NAcore cells were visualized using differential interference contrast (DIC) through a 40x liquid-immersion objective mounted on an upright light microscope (Olympus, BX-RFA). NAcore MSNs expressing mCherry were visualized using an integrated green LED (545 nm;  $<1$  mW). Whole-cell recordings were obtained using borosilicate pipettes (3–7 M $\Omega$ ) back-filled with Cesium methanesulfonate, which contained (in mM): 117 Cs methanesulfonic acid, 20 HEPES, 10 EGTA, 2 MgCl<sub>2</sub>, 2 ATP, 0.2 GTP (pH 7.35, mOsm 280).

Voltage-clamp recordings were obtained from mCherry<sup>+</sup> and neighboring mCherry<sup>-</sup> NAcore MSNs to characterize inputs from PrL. During recordings, NAcore MSNs were held at  $-70$  mV and PrL axons containing AAV2-EF1a-DIO-hChR2-EYFP were activated through a 10 ms pulse of a blue LED (470 nm; 1 mW) delivered every 5 s. Importantly, the exact same stimulation parameters were kept throughout all recordings. The resulting optogenetically evoked EPSCs were recorded and peak amplitudes were analyzed using Clampfit (v10).

## In vivo Electrochemistry

*In vivo* electrochemical detection and quantification of glutamate levels were performed as previously described (Siemsen et al., 2020). Following SA, surgery, abstinence, and extinction, Glutamate oxidase (GluOx)-coated electrochemical electrodes were implanted (Pinnacle Technology, Lawrence, KS, United States) and connected to a wireless potentiostat housed within a 3D-printed enclosure; data was transmitted from the potentiostat via Bluetooth. Electrodes were calibrated and implanted as described previously (Siemsen et al., 2020). Following implantation animals were returned to the colony overnight. The next morning, a  $\sim 1$ -h baseline recording began; animals undergoing cocaine seeking were injected with CNO (5 mg/kg, i.p.) 30 min prior to the reinstatement session. Animals undergoing sucrose seeking did not receive CNO. One Hz measurements of glutamate-dependent currents were expressed relative to a 15-min pre-session baseline, then converted to glutamate concentrations (in nM) based off the *in vitro* calibration. While behavioral testing lasted two hours, recordings were stopped after the first hour. Animals were perfused following testing. Virus expression and probe placement were mapped according to the atlas of Paxinos and Watson.

## Microscopy

Detailed methods regarding virus vector mapping, cell counting, and Fos imaging and analyses can be found in the **Supplementary Information**.

## Dendritic Spine and Astrocyte Membrane Imaging

Eighty-micron ( $\mu\text{m}$ ) coronal sections were immunohistochemically processed for Flag (to label neurons) and GFP (to label astrocytes) and imaged using a Leica SP8 laser-scanning confocal microscope. NAc<sub>core</sub> neurons receiving PrL input and surrounding astrocytes were imaged with an OPAL 552 nm and an Argon 488 nm laser line, respectively. Dendrites were selected for imaging based off the following criteria: (1) relative isolation from interfering dendrites, (2) location past the second branch point from the soma, (3) traceability back to a soma of origin, and (4) location within a field of labeled astrocytes. Images were acquired using a 63X oil-immersion objective (1.4 N.A.) with a frame size of  $1024 \times 512$  pixels, a step size of  $0.1 \mu\text{m}$ , 4.1X digital zoom, and a 0.8 AU pinhole. Laser power and gain were optimized then held relatively constant only adjusting to maintain voxel saturation consistency between images. Images were deconvolved using Huygens software (Scientific Volume Imaging, Hilversum, Netherlands) prior to analyses.

## Imaris Analyses

### Dendritic Spine Morphometrics and Astrocyte Association at Dendritic Spine Heads

Deconvolved Z-stacks were imported to Imaris. Dendritic spine analyses were performed as previously described (Siemsen et al., 2018a). Briefly, the filament tool was used to trace the dendrite shaft and spines. The average diameter ( $d_H$ ,  $\mu\text{m}$ ) of spine heads on each dendrite, as well as the dendritic spine density (number of spines per  $\mu\text{m}$  of dendrite) were exported.

To analyze astrocyte association with spines (**Supplementary Figure S1**), the filament analysis extension was used to model dendritic spine heads as spheres, which were converted to rendered surfaces. Next, the dilate surface extension was used to expand each dendritic spine head surface by 300 nm, producing a hollow expanded sphere for each spine head. Next, an automatic threshold was used to render the volume of astrocyte membrane within each hollow sphere ROI. The physical volume of astrocyte signal within each hollow sphere ROI surrounding the spine head was normalized to the corresponding volume of each hollow sphere, yielding a % association for each spine head. This allows equivalent analyses of astrocyte association with dendritic spine heads, independent of the size of the spine head. Average GFP intensity within the ROI, % of spines along the dendrite with 0 association, the average % association at spine heads, as well as the % association at each individual spine head on the dendrite were assessed.

## Statistical Analyses

All statistical analyses were performed with GraphPad Prism (v9) software. When comparing groups across time or bins a mixed-effects model (for missing values) or mixed-model two-way ANOVA with virus or treatment as a between subject variable

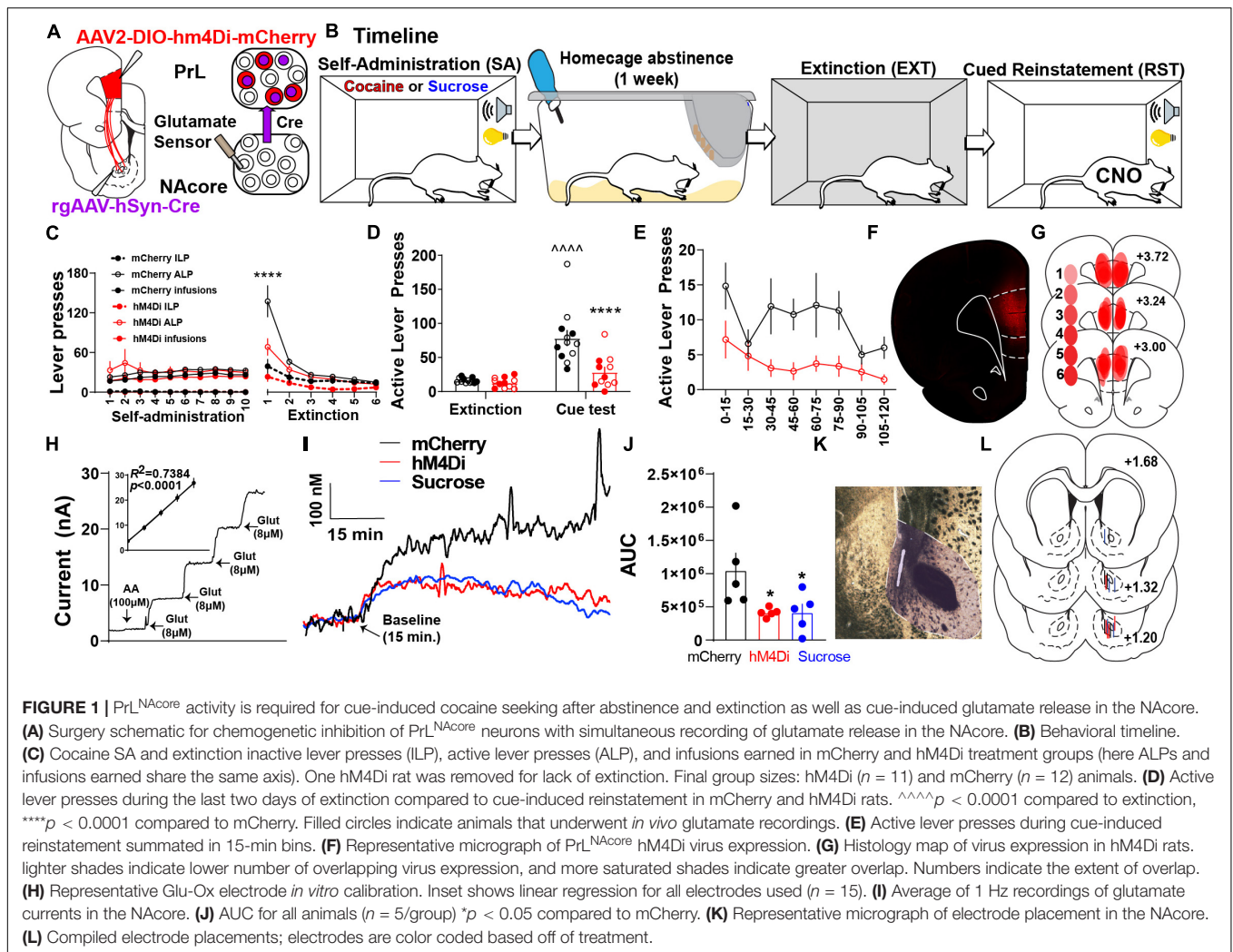
and session/test/bin as the within subject variable followed by Bonferroni-corrected multiple comparison test when an interaction or main effect was significant. Fos data were analyzed with a two-way ANOVA with virus (mCherry vs. hM4Di) and reward (cocaine vs. sucrose) as between subject variables followed by Tukey's multiple comparison tests when an interaction was significant. Correlation analyses were performed using a two-tailed Pearson's correlation. Electrochemical calibration data was analyzed with linear regression and changes in glutamate concentrations during reinstatement were analyzed using area under the curve (AUC) analyses. AUC's were then compared across groups using a one-way ANOVA with a Dunnett's multiple comparison test. Paired and unpaired observations were analyzed with a paired or un-paired, with the appropriate correction if needed, *t*-test, respectively. Significance was set at  $p < 0.05$  and data is expressed as the mean  $\pm$  the standard error of the mean. All non-significant behavioral data is presented in **Supplementary Table S1**.

## RESULTS

### Chemogenetic Inhibition of PrL<sup>NAcore</sup> Neurons Suppresses Cue-Induced Reinstatement and Associated Glutamate Release in the Nucleus Accumbens Core

To test whether PrL neurons projecting to the NAc<sub>core</sub> (PrL<sup>NAcore</sup>) are required for cue-induced reinstatement and increased glutamate release in the NAc<sub>core</sub>, we expressed inhibitory hM4Di-DREADDs in PrL<sup>NAcore</sup> neurons using an intersectional chemogenetic approach (**Figure 1A**). Animals underwent cocaine or sucrose SA, followed by one week of home cage abstinence, then extinction training (**Figure 1B**). Following cocaine or sucrose SA, 7-day home-cage abstinence, and extinction training (**Figure 1C** and **Supplementary Figure S2**). Within **Figure 1C**, both ALPs and infusions earned share the same axis. Animals were then administered CNO 30 min prior to the presentation of cocaine-paired cues. Cocaine seeking was then measured as the number of non-reinforced presses of the lever formerly paired with cocaine (i.e., "active" lever presses or ALPs). Comparing the last day of extinction, cue presentation to DIO-mCherry control animals produced a significant increase in drug seeking on the active lever [two-way mixed-model ANOVA, significant group by test interaction,  $F(1,21) = 11.73$ ,  $p = 0.003$ , **Figure 1D**], which was suppressed in the DIO-hM4Di rats compared to mCherry controls ( $p < 0.0001$ ). When ALPs during reinstatement were summated in 15 min bins, there was a main effect of group [ $F(1,21) = 12.60$ ,  $p = 0.002$ , **Figure 1E**], indicating that ALPs were lower in hM4Di compared to mCherry rats regardless of the time bin. Representative PrL<sup>NAcore</sup> hM4Di expression is shown in **Figure 1F** and a compiled histology map for hM4Di rats is shown in **Figure 1G**.

In a subset of the cocaine SA animals, we also examined the influence of PrL<sup>NAcore</sup> neurons on cue-induced glutamate release in the NAc<sub>core</sub>. Extracellular glutamate levels were detected using



a calibrated GluOx-coated electrode implanted in the NAcore (Figures 1A,H) and cued glutamate release was measured in cocaine (mCherry and hM4Di) and sucrose reinstating rats (Figure 1I). When analyzing the area under the curve (AUC) of 1 Hz measurements of glutamate release in the three groups, we detected a main effect of cue on NAcore glutamate levels [one-way ANOVA, main effect of treatment,  $F(2,12) = 4.55$ ,  $p = 0.034$ , Figure 1J]. Compared to PrL<sup>NAcore</sup> DIO-mCherry controls, the PrL<sup>NAcore</sup> DIO-hM4Di animals and animals reinstating to sucrose-paired cues both showed a significant reduction in cue-induced glutamate release in the NAcore ( $p = 0.04$ ).

## AAV1-CamKII $\alpha$ -Cre Injections in the Prelimbic Cortex Transduce a Subpopulation of Nucleus Accumbens Core Neurons Receiving Dense Prelimbic Cortical Input

Like other AAV serotypes, AAV1 viral particles transduce neurons in the primary injection site. However, one unique property of AAV1 vectors is that a portion of viral particles are

trafficked anterogradely down axons then released via vesicle fusion at axon terminals. This allows for transfer of viral particles and transgene expression in downstream neurons receiving synaptic contacts (Zingg et al., 2017, 2020). Importantly, AAV1-mediated transsynaptic transduction is monosynaptic (Oh et al., 2020) and strongest and strongest in neurons that receive numerous functional inputs from cells at the primary injection site, with the original characterization of these vectors and their anterograde transsynaptic transfer demonstrating a significant association between postsynaptic AAV transduction and presynaptic connectivity (Zingg et al., 2017, 2020). As such, we took advantage of this characteristic of AAV1 vectors to investigate NAcore neurons receiving dense and functional PrL inputs (NAcore<sup>PrL</sup>). First, we determined what percentage of NAcore neurons are transduced via AAV1 transsynaptic transduction by infusing AAV1-CamKII $\alpha$ -Cre in the PrL cortex and AAV1-CAG-Flex-Ruby2sm-Flag (Flex-smFP) or AAV2-hSyn-DIO-hM4Di-mCherry in the NAcore (Figures 2A–C). Within the field of viral transduction in the NAcore,  $\sim 10\%$  of the neurons were labeled (Figure 2D). Further analysis of NAcore<sup>PrL</sup> neurons revealed that a large fraction of NAcore<sup>PrL</sup>

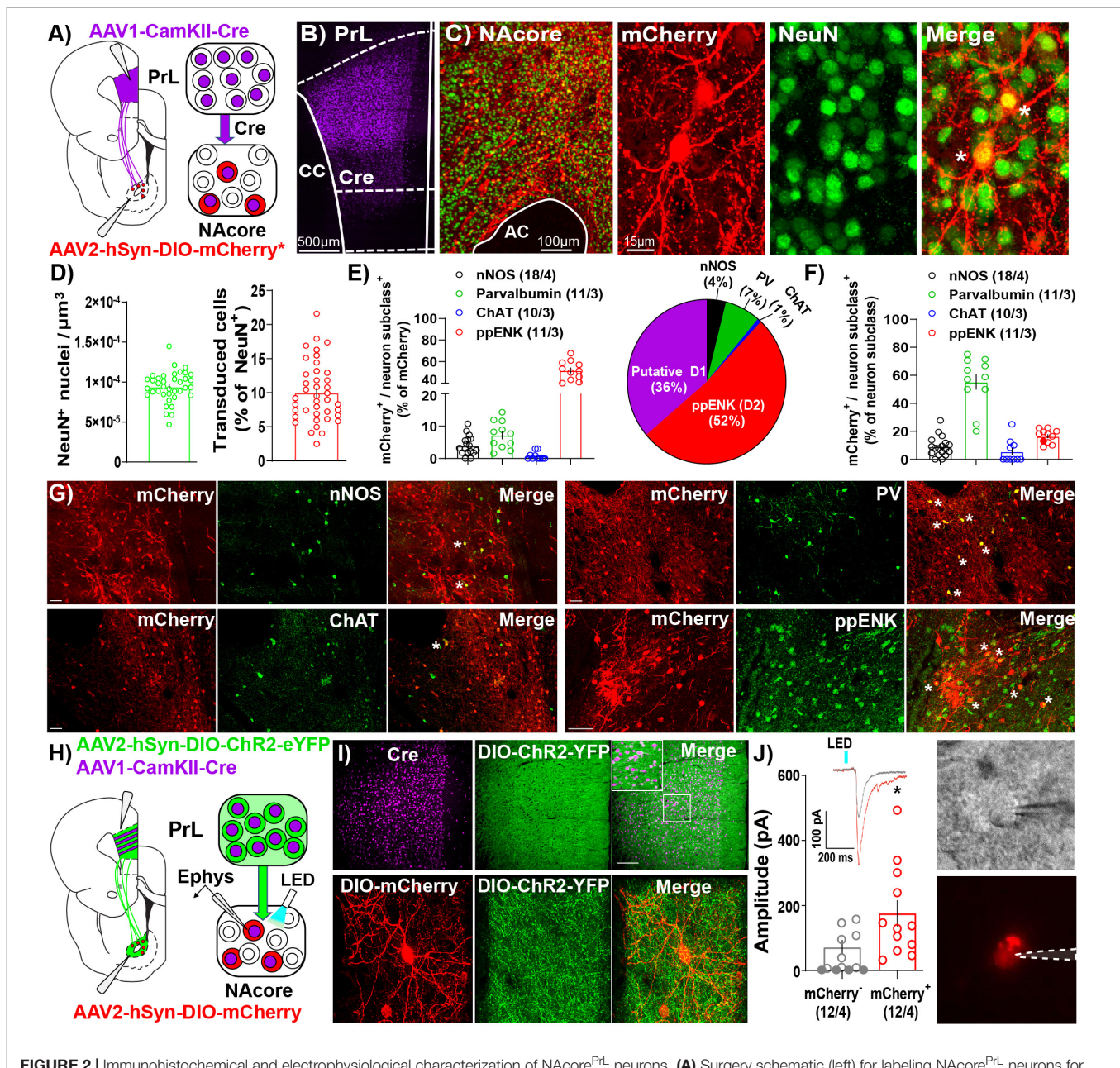


**FIGURE 2 |** Immunohistochemical and electrophysiological characterization of NAcore<sup>PrL</sup> neurons. **(A)** Surgery schematic (left) for labeling NAcore<sup>PrL</sup> neurons for manipulation. Asterisk indicates use of DIO-hm4Di-mCherry or Flex-smFP for analyses. **(B)** Representative confocal image of immunohistochemically detected Cre (from AAV1-CamKII $\alpha$ -Cre) in the first-order region (PrL cortex). **(C)** Representative image of NeuN (green) and Flag-tagged Flex-smFP (red) in the NAcore. High magnification image is shown to the right. **(D)** Left – NeuN<sup>+</sup> nuclei normalized to dataset volume ( $\mu$ m<sup>3</sup>). Right – Percent of NeuN nuclei that were transduced by AAV1-CamKII $\alpha$ -Cre in the PrL cortex and Cre-dependent vectors in the NAcore from three groups of rats, animals expressing Flex-smFP in NAcore<sup>PrL</sup> neurons that underwent yoked-saline (11 images from 3 animals), 15 min of cocaine seeking (12 images from 3 animals), or animals undergoing 2 h of cue-induced reinstatement with hm4Di expression in NAcore<sup>PrL</sup> neurons (17 images from 3 animals). **(E)** Left – Percent of NAcore<sup>PrL</sup> neurons that were co-labeled by nNOS, Parvalbumin (PV), Choline acetyltransferase (ChAT), or pre-pro enkephalin (ppENK). Right – Pie chart summarizing data in **(E)**. **(F)** Percent of each neuron subclass that was also mCherry<sup>+</sup> (inverse of data in **E**). Representative images of mCherry/nNOS (top, left-scale bar = 100  $\mu$ m), mCherry/ChAT (bottom, left-scale bar = 100  $\mu$ m), mCherry/PV (top, right-scale bar = 100  $\mu$ m), and mCherry/ppENK (bottom, right-scale bar = 50  $\mu$ m). Tissue was processed from animals expressing DIO-hm4Di in NAcore<sup>PrL</sup> neurons undergoing 2 h of cue-induced reinstatement ( $n = 3-4$  animals). **(G)** Representative images from cell type identification analyses. **(H)** Schematic of slice electrophysiology during optogenetic stimulation of PrL terminals in the NAcore. **(I)** Representative images of immunohistochemically detected Cre in the PrL cortex (top, left), DIO-hChR2-EYFP (top, middle), and merge of the two signals (top, right) in the PrL cortex following an injection of AAV1-CamKII $\alpha$ -Cre and AAV2-EF1a-DIO-hChR2-EYFP ( $n = 4$  rats). Scale bar = 200  $\mu$ m (top, main), 50  $\mu$ m (inset). A representative DIO-mCherry-labeled NAcore<sup>PrL</sup> neuron (bottom, left), axonal fibers from DIO-hChR2-EYFP in the NAcore (bottom, middle), and merge of the two signals (bottom, right) is shown below. Scale bar = 30  $\mu$ m. **(J)** Left – EPSC amplitude in mCherry<sup>-</sup> and mCherry<sup>+</sup> cells following optogenetic stimulation of PrL terminals in the NAcore. Inset shows representative traces from the two cell types. Right – Representative DIC (top) and fluorescent filtered (bottom) mCherry<sup>+</sup> cell chosen for patching. \* $p < 0.05$  compared to mCherry<sup>-</sup>.

neurons exhibited reactivity for pre-pro Enkephalin (ppENK), a marker for D2 MSNs (Lu et al., 1998), whereas a smaller subset exhibited reactivity for various interneuron markers (Figure 2E). As CamKII $\alpha$  expression has been demonstrated in both MSNs (Klug et al., 2012) and interneurons (Keaveney et al., 2020), the transsynaptic transduction in these downstream targets observed here is consistent with these observations. Moreover, the CamKII $\alpha$  promoter was selected to avoid transduction of long range PrL to NAc core GABAergic projections (Lee et al., 2014). Interestingly, even though a minority of NAc core<sup>PrL</sup> neurons were identified as parvalbumin interneurons (PV), we found ~60% of total NAc core PV neurons were transduced via their inputs from the PrL (Figure 2F). Representative images for each immunohistochemical cell type identification experiment are shown in Figure 2G.

In a separate cohort of drug-naïve rats, we co-injected AAV1-CamKII $\alpha$ -Cre and AAV2-EF1a-DIO-hChR2-EYFP into the PrL cortex and AAV2-hSyn-DIO-mCherry in the NAc core and used

a blue light-evoked EPSC protocol (Otis et al., 2019) to record EPSC amplitude in mCherry<sup>+</sup> and neighboring mCherry<sup>-</sup> neurons in the NAc core (Figures 2H,I). Fifty-eight percent of mCherry<sup>-</sup> neurons either showed no response (33%), or a response < 10 pA (25%), whereas 100% of mCherry<sup>+</sup> cells responded (see Table 2). When removing mCherry<sup>-</sup> cells that showed no response, mCherry<sup>+</sup> cells showed a greater EPSC amplitude compared to mCherry<sup>-</sup> cells [Welch's-corrected *t*-test,  $t(16.34) = 2.259$ ,  $p = 0.038$ , Figure 2J].

## Chemogenetic Inhibition of NAc core<sup>PrL</sup> Neurons Suppresses Cue-Induced Reinstatement of Cocaine, but Not Sucrose, Seeking

To examine the contribution of NAc core<sup>PrL</sup> neurons in reward-seeking behavior, we microinjected AAV1-CamKII $\alpha$ -Cre into the PrL cortex and AAV2-hSyn-DIO-hM4Di-mCherry or

**TABLE 2** | Electrophysiology data.

mCherry(-)							
Neuron	PrL Input	Response	Peak Amp	Membrane	Data Summary		
	(mCherry +)	To Stim	Avg (pA)	Resistance (Rm)		mCherry (+)	Unlabeled
O1N2	No	No	0	154	Response Rate (%)	100	66.66666667
O1N4	No	No	0	190			
O2N3	No	Yes	-8.5	1000	Peak Amp (pA)	<b>Average</b>	<b>Average</b>
O2N5	No	Yes	-95.69	120		-176.0008333	-47.68
O3N5	No	Yes	-146.25	145	Peak Amp (pA)	<b>SEM</b>	<b>SEM</b>
O3N6	No	Yes	-157.96	170		40.49380161	17.7547845
O3N10	No	Yes	-107.81	345	<b>t-test peak amp</b>	<b>p-value</b>	<b>Result</b>
O3N8	No	No	0	150		0.038	Significant
O5N1	No	Yes	-39.49	280	<b>t-test Rm</b>	0.269670548	No Significance
O5N7	No	No	0	480			
O5N8	No	Yes	-6.8	1100			
O5N9	No	Yes	-9.66	340			
<b>Average</b>			-47.68	372.83			
<b>SEM</b>			17.75	96.61			
mCherry (+)							
Neuron	PrL Input	Response	Peak Amp	Membrane			
	(mCherry+)	To Stim	Avg (pA)	Resistance (Rm)			
O1N1	Yes	Yes	-80.22	120			
O2N1	Yes	Yes	-146.9	400			
O2N2	Yes	Yes	-60.82	120			
O2N4	Yes	Yes	-129.09	400			
O3N1	Yes	Yes	-301	160			
O3N2	Yes	Yes	-239.86	127			
O3N3	Yes	Yes	-493.32	180			
O3N9	Yes	Yes	-32.26	440			
O5N2	Yes	Yes	-137.98	275			
O5N3	Yes	Yes	-105.29	260			
O5N4	Yes	Yes	-339.1	350			
O5N5	Yes	Yes	-46.17	250			
<b>Average</b>			-176.00	256.83			
<b>SEM</b>			40.49	34.07			

PrL = prelimbic, Amp = amplitude, Avg = average, pA = picoamps, Rm = membrane resistance, SEM = standard error of the mean.

AAV2-hSyn-DIO-mCherry into the NAc<sub>core</sub> (Figure 3A). Animals underwent cocaine or sucrose SA, extinction, and cue-induced reinstatement (Figure 3B). AAV1-CamKII $\alpha$ -Cre injections were confined to the PrL cortex, and AAV2-DIO-hM4Di transduced a subpopulation of cells in the NAc<sub>core</sub> (Figures 3C,D). Importantly, throughout all experimentation, expression of DIO-mCherry or DIO-hM4Di was confirmed to be restricted to the core subregion of the nucleus accumbens (see Figure 3D inset panel), given that a small population of PrL neurons do exist that send input the shell subcompartment of the nucleus accumbens (Wayman and Woodward, 2018a). Animals that were infused with either DIO-mCherry or DIO-hM4Di were taken through cocaine self-administration and extinction (Figure 3E) and both reinstated to cocaine-paired cues [two-way mixed-model ANOVA, group by test interaction,  $F(1,21) = 13.94$ ,  $p = 0.001$ ; mCherry ( $p < 0.0001$ ), hM4Di ( $p = 0.006$ ), Figure 3F]. Compared to mCherry controls, the chemogenetic inhibition of NAc<sub>core</sub><sup>PrL</sup> neurons reduced cue-induced reinstatement ( $p < 0.0001$ ), which was most pronounced during the first 30 min of the cue test when ALP data was binned into 15-min time blocks [two-way RM ANOVA, virus by time point interaction,  $F(7,147) = 3.743$ ,  $p = 0.0009$ , Figure 3G] and significant differences between mCherry and hM4Di were observed at 15 ( $p < 0.0001$ ) and 30 min ( $p < 0.05$ ) minutes. Interestingly, for DIO-mCherry and DIO-hM4Di rats undergoing sucrose self-administration and extinction (Figure 3H), there was a main effect of cued sucrose seeking [two-way mixed model ANOVA,  $F(1,14) = 46.03$ ,  $p < 0.0001$ , Figure 3I], yet NAc<sub>core</sub><sup>PrL</sup> inhibition did not affect cue-induced reinstatement. There was also no difference in cued sucrose seeking with NAc<sub>core</sub><sup>PrL</sup> inhibition when ALP data was binned [two-way RM ANOVA,  $F(7,98) = 0.82$ ,  $p = 0.573$ , Figure 3J], indicating that NAc<sub>core</sub><sup>PrL</sup> neurons are required for cued seeking for cocaine, but not sucrose rewards.

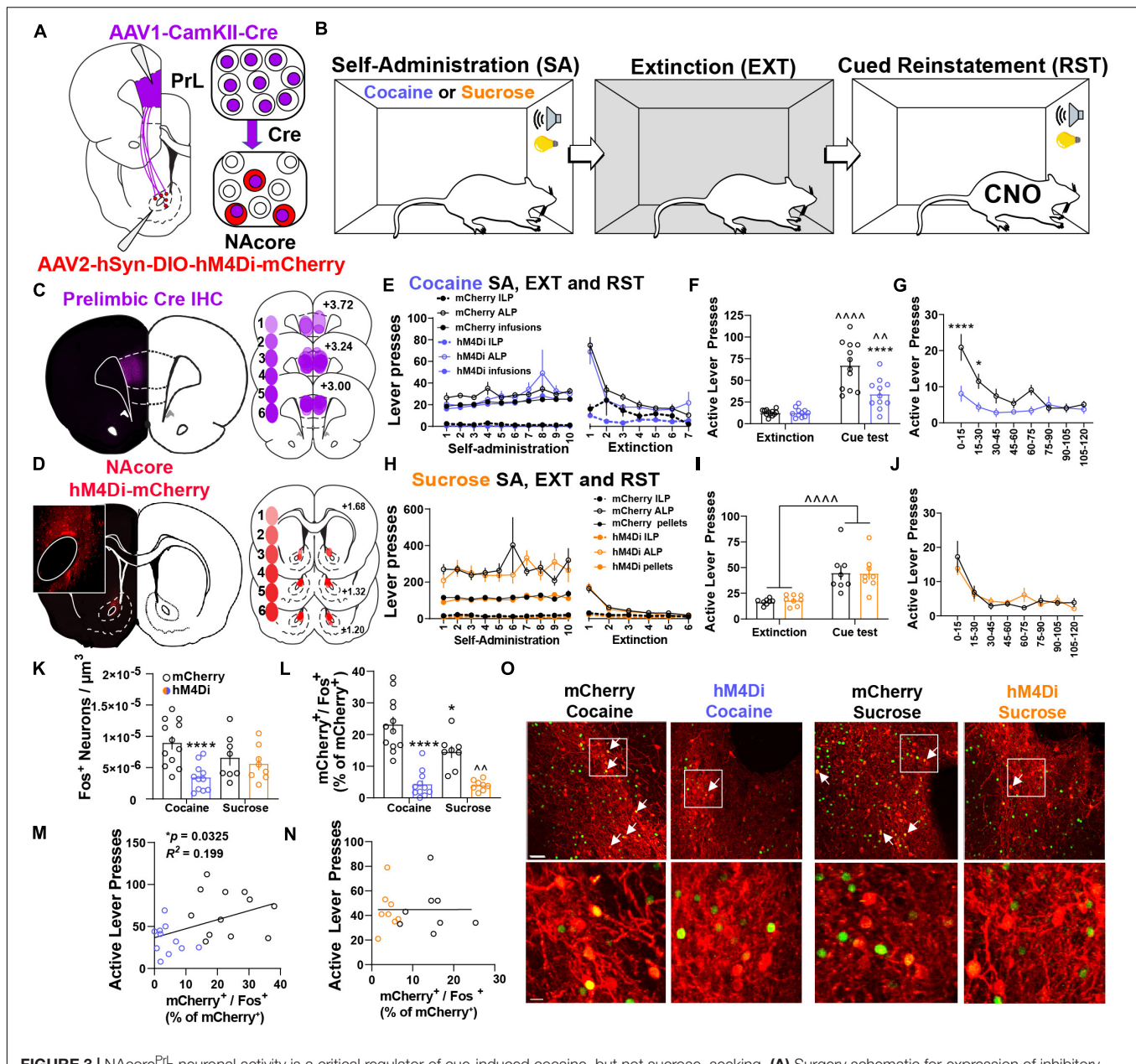
Next, we used Fos immunoreactivity to examine neuronal activation in the NAc<sub>core</sub> following cued reinstatement of cocaine or sucrose seeking. Compared to yoked-saline controls sacrificed 24 h after the last extinction session, cued seeking in virus control animals (mCherry-Cocaine and mCherry-sucrose) produced a significant increase in Fos staining in the NAc<sub>core</sub>, which included NAc<sub>core</sub><sup>PrL</sup> neurons (Supplementary Figure S3). When also including cue-induced Fos staining in the hM4Di-Cocaine and hM4Di-sucrose groups, a significant interaction between reward and virus was observed [two-way ANOVA,  $F(1,35) = 5.178$ ,  $p = 0.029$ , Figure 3K]. Compared to mCherry-Cocaine animals, only hM4Di-Cocaine animals showed reduced Fos in the NAc<sub>core</sub> overall ( $p = 0.0007$ ). When limiting the analysis to NAc<sub>core</sub><sup>PrL</sup> neurons, a two-way ANOVA revealed a significant reward by virus interaction [ $F(1,35) = 4.746$ ,  $p = 0.036$ , Figure 3L]. Compared to mCherry-Cocaine rats, all other groups showed reduced Fos expression in NAc<sub>core</sub><sup>PrL</sup> neurons ( $p$ 's  $< 0.05$ ). As expected, hM4Di-Sucrose rats showed reduced Fos expression in NAc<sub>core</sub><sup>PrL</sup> neurons compared to mCherry-Sucrose ( $p = 0.005$ ). Interestingly, ALPs during reinstatement positively correlated with Fos activation in

NAc<sub>core</sub><sup>PrL</sup> neurons in cocaine ( $r = 0.447$ ,  $p = 0.033$ , Figure 3M), but not sucrose animals ( $r = 0.002$ ,  $p = 0.992$ , Figure 3N). Representative images for Fos quantification analyses are shown in Figure 3O.

### NAc<sub>core</sub><sup>PrL</sup> Medium Spiny Neurons Undergo Transient Structural Plasticity and Increased Astrocyte Association at Dendritic Spines During Reinstatement

Given NAc<sub>core</sub><sup>PrL</sup> neurons are necessary for cued drug seeking, we next asked whether NAc<sub>core</sub><sup>PrL</sup> dendritic spine heads and surrounding perisynaptic astrocyte processes (PAPs) undergo morphological plasticity during cued cocaine seeking. To label NAc<sub>core</sub><sup>PrL</sup> neurons and surrounding astrocytes, we microinjected AAV1-CamKII $\alpha$ -Cre in the PrL cortex and a mix of AAV1-CAG-Flex-Ruby2sm-Flag to label dendritic spines and AAV5-GfaABC1D-Lck-GFP to label astrocyte PAPs in the NAc<sub>core</sub> (Figure 4A). Following cocaine SA and extinction training, animals were sacrificed 15 min into cue-induced reinstatement (cocaine), and these were compared to yoked-saline control animals sacrificed 24 h after extinction (Figure 4B). There was no difference in the percent of transduced neurons in the NAc<sub>core</sub> between cocaine and yoked saline rats [ $t(21) = 0.794$ ,  $p = 0.436$ , Figure 2D], or in the percentage of NAc<sub>core</sub><sup>PrL</sup> neurons that were ppENK<sup>+</sup> (Supplementary Figure S4). Akin to prior experiments, CamKII $\alpha$ -driven Cre expression in the primary injection site was confined to the PrL cortex and Flex-Ruby2sm-Flag provided sparse, fully labeled NAc<sub>core</sub> neurons, including MSNs (identified via their morphological signature) for spine analyses (Figures 4C,D). Following cocaine SA and extinction training (Figure 4E), we observed that cued reinstatement significantly increased dendritic spine head diameter ( $d_H$ ) of NAc<sub>core</sub><sup>PrL</sup> spines [paired  $t$ -test,  $t(115) = 5.780$ ,  $p < 0.0001$ , Figure 4F]. This increase in  $d_H$  was associated with a rightward shift in dendritic spine  $d_H$  when spine  $d_H$  was binned to generate a frequency distribution. While the area under the curve for the spine head data presented in Figure 4G is similar for control and cocaine seeking animals our data indicate a rightward shift in the frequency distribution of dendritic spine heads during cue-induced cocaine seeking, indicating an increase in the frequency of large spine heads and a decrease in frequency of smaller spine heads [two-way mixed model ANOVA, group by bin interaction,  $F(5,575) = 13.22$ ,  $p < 0.0001$ , Figure 4G], with no change in spine density [ $t(115) = 0.905$ ,  $p = 0.367$ , Figures 4H,I].

Next, we evaluated whether astrocyte PAPs undergo morphological plasticity at dendritic spine heads of NAc<sub>core</sub><sup>PrL</sup> MSNs during seeking and whether this occurs at specific subsets of spines (Figure 4J and Supplementary Figure S1A). Interestingly, compared to yoked-saline controls, cue-induced cocaine seeking animals had a significantly lower percent of spines without any astroglial association [Welch's-corrected two-tailed  $t$ -test,  $t(80.07) = 3.933$ ,  $p = 0.0002$ , Figure 4K], and the average astroglial association with dendritic spine heads on NAc<sub>core</sub><sup>PrL</sup> neurons was significantly increased



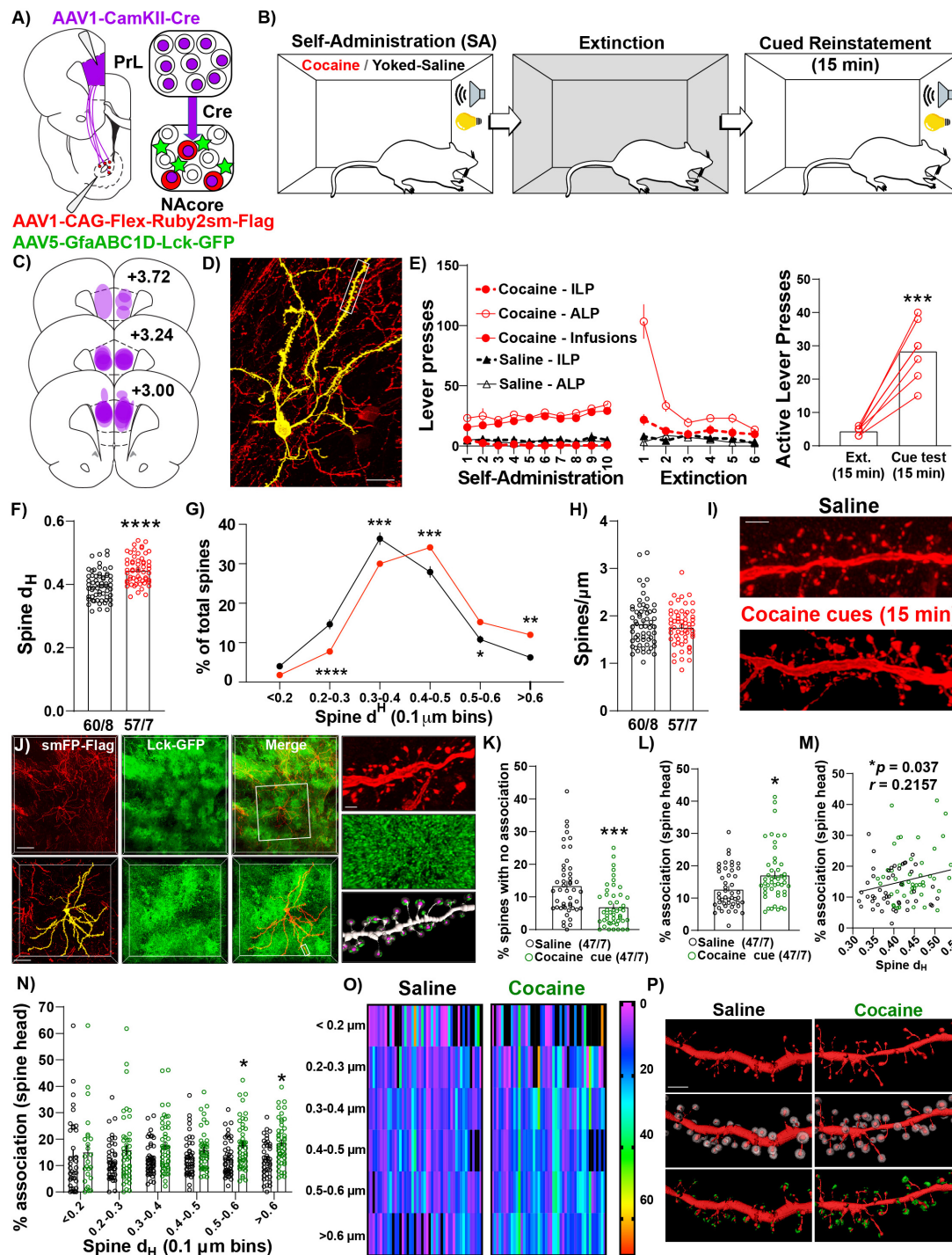


**FIGURE 4** | NAcCore<sup>PrL</sup> neurons undergo the structural component of transient potentiation which is associated with enhanced astrocyte association at spines during cue-induced reinstatement. **(A)** Surgical schematic for labeling NAcCore<sup>PrL</sup> neurons for dendritic spine morphology and astrocyte association imaging. **(B)** Behavioral timeline. One cocaine animal was removed for off-target virus expression. Animals either underwent cocaine SA ( $n = 7$ ) or received yoked saline infusions ( $n = 8$ ), extinction, and cocaine SA animals underwent cue-induced reinstatement for 15 min. **(C)** Histology map of viral spread in the PrL cortex revealed by Cre immunohistochemistry. **(D)** Representative Flex-smFP labeled NAcCore<sup>PrL</sup> MSN in the NAcCore. **(E)** ILP, ALP, and infusions earned for cocaine SA and yoked saline rats during SA and extinction (left) and active lever presses during the 15 min of cue-induced reinstatement compared to the first 15 min of the last extinction session (right); \*\*\* $p < 0.001$  compared to extinction. **(F)** Dendritic spine head diameter ( $d_H$ ) was increased at 15 min of reinstatement in cocaine SA animals compared to yoked saline animals sacrificed at an extinction baseline (Yoked saline – 60 dendrite segments from 8 animals; cocaine – 57 segments from 7 animals); \*\*\*\* $p < 0.0001$  compared to yoked saline. **(G)** Frequency distribution of binned dendritic spine  $d_H$  showing a general rightward shift in the distribution in cocaine

(Continued)

**FIGURE 4** | reinstating animals. \* $p < 0.05$ , \*\* $p < 0.01$ , \*\*\* $p < 0.001$ , \*\*\*\* $p < 0.0001$  compared to yoked saline. **(H)** There was no difference in dendritic spine density between groups. **(I)** Representative dendritic spine segments from yoked saline and cocaine cue reinstating rats. Scale bar = 2  $\mu\text{m}$ . **(J)** Representative image of Flag-tagged Ruby2sm-labeled NAc<sup>PrL</sup> MSN and surrounding Lck-GFP-labeled astrocytes (top, scale bar = 100  $\mu\text{m}$ ) and high magnification inset (bottom, scale bar = 50  $\mu\text{m}$ ) of boxed region in top panel. Right-High magnification image of boxed region in bottom left panel showing a dendritic spine segment (top, scale bar = 2  $\mu\text{m}$ ), Lck-GFP (middle), and Lck-GFP (green) confined to the region surrounding each dendritic spine head (purple) across the dendrite. **(K,L)** For astrocyte interaction analyses, one yoked saline animal was removed from association analyses due to weak Lck-GFP virus expression relative to all other animals ( $n = 8$  segments). An additional 5 segments were removed from the yoked saline group, and 10 were removed from the cocaine group, due to either uneven Lck-GFP intensity across the dendrite or because the imaged astrocyte only ensheathed  $\leq 50\%$  of the dendrite. Cue-induced reinstatement of cocaine seeking decreases the percent of dendritic spines that have no association **(K)**, while increasing the average percent association across the dendrite **(L)**. \* $p < 0.05$ , \*\*\* $p < 0.001$  compared to yoked saline. **(M)** The percent association positively correlated with the average dendritic spine  $d_H$ . **(N)** Percent association as a function of spine  $d_H$  separated by spine size bin. \* $p < 0.05$  compared to yoked saline. **(O)** Heat map of data in N. Warmer colors indicate greater percent astrocyte association. In this instance, black refers to either 0 percent association or a bin with no spines. Each dendrite sampled is represented as 1 column. **(P)** Representative NAc<sup>PrL</sup> dendrites sampled (top), the same dendrite with expanded region surrounding each spine (middle), and astrocyte membrane physical volume confined to the region surrounding each spine head (bottom). **(F–H,K–O)** Each data point represents the average value for an individual dendrite.

during cocaine seeking (Mann–Whitney test,  $U = 781$ ,  $p = 0.014$ , **Figure 4L**), which positively correlated with the dendrites' average spine  $d_H$  ( $r = 0.216$ ,  $p = 0.037$ , **Figure 4M**). We also examined which NAc<sup>PrL</sup> spines showed the increased astroglial association. When analyzing the astroglial association across binned spine head sizes (**Figures 4N–P**), we observed a main effect of cue [ $F(1,92) = 7.08$ ,  $p = 0.009$ ] and an increase in the percent astrocyte association with the largest NAc<sup>PrL</sup> spines (Bonferroni *post hoc*,  $0.5\text{--}0.6 \mu\text{m} - p = 0.049$ ,  $>0.6 \mu\text{m} - p = 0.023$ ). Importantly, these effects were not due to differences in the intensity of GFP in the astrocyte processes (**Supplementary Figure S1B**).

We also asked whether these adaptations occur 24 h after the last SA session given that repeated cocaine increases basal dopamine concentrations in the NAc 24 h after the final injection (Weiss et al., 1992) without altering dendritic spine density on distal dendrites of NAc MSNs (Dumitriu et al., 2012), and astrocytes respond to synaptically released dopamine by increasing  $\text{Ca}^{2+}$  mobility to drive gliotransmission (Corkrum et al., 2020), a phenomenon often paired with increased PAPs association at synapses (Bernardinelli et al., 2014). Akin to previous findings regarding spine density 24 h after repeated daily cocaine injections (Dumitriu et al., 2012), dendritic spine density or head diameter of NAc<sup>PrL</sup> neurons was unaltered 24 h after cocaine SA and no changes in astrocyte-dendritic spine association were observed (**Supplementary Figures S5A–G**).

## DISCUSSION

Here we showed that PrL<sup>NAcore</sup> neurons are required for cue-induced cocaine seeking and associated glutamate release in NAc. Moreover, we found that a small subpopulation of NAc<sup>PrL</sup> neurons (recruited by input and density-dependent AAV1 transsynaptic transduction from the PrL cortex) are necessary for cue-induced cocaine, but not sucrose, seeking. Importantly, these neurons undergo the structural component of transient synaptic potentiation during reinstatement, as indicated by increased dendritic spine  $d_H$  and enhanced astrocyte association with large spines at the peak of responding for cocaine cues. These data demonstrate that NAc<sup>PrL</sup> neurons

represent a crucial subset of neurons linked to cocaine, and not sucrose, seeking.

## Role of PrL<sup>NAcore</sup> Neurons in Cocaine Seeking and Nucleus Accumbens Core Glutamate Release

Previous findings have indicated a clear role for PrL<sup>NAcore</sup> neurons in driving cued cocaine seeking, but not food seeking, via glutamate release in the NAc (Gipson et al., 2013a; Scofield et al., 2016a; Stefanik et al., 2016). Alternatively, activation of infralimbic to nucleus accumbens shell neurons has been shown to reduce cue-induced cocaine seeking (Peters et al., 2008; Augur et al., 2016). While glutamate release in the nucleus accumbens is thought to drive these effects, evidence exists that recruitment of the PrL neurons that supply excitatory input to the NAc requires DA release in the PrL (McGlinchey et al., 2016; James et al., 2018). Moreover, while our manipulations were restricted to the PrL and its input to the NAc, it is also important to note that glutamate release from neurons located in the adjacent infralimbic cortex can also influence extracellular dopamine levels in the shell subcompartment of the nucleus accumbens through infralimbic-mediated activation of dopamine neurons in the ventral tegmental area (Quiroz et al., 2016). Despite what is currently known, the contribution of PrL-dependent glutamate release in the NAc has yet to be directly compared between cocaine and sucrose reinstating animals. Our study is the first to demonstrate in real time that chemogenetic inhibition of PrL<sup>NAcore</sup> neurons suppresses both cue-induced seeking and the associated elevations in NAc glutamate release. We find that chemogenetic inhibition of PrL<sup>NAcore</sup> neurons normalized cue-induced glutamate release in the NAc to levels that were nearly identical to those observed in animals undergoing sucrose seeking. Thus, PrL<sup>NAcore</sup> neurons represent a primary source of cue-induced glutamate release in the NAc to drive cocaine seeking.

Conversely, it has been demonstrated that inhibition of the infralimbic cortex prevents appetitive eating and fearful behaviors precipitated by disruption of glutamatergic signaling in the nucleus accumbens shell (Richard and Berridge, 2013). Speaking to a potential PrL and infralimbic dichotomy, following exposure to the inhalant Toluene and a single day of withdrawal, decreased intrinsic excitability in layer 5/6 PrL neurons that

project to the NAc core and increased intrinsic excitability in infralimbic neurons (in either Layer 2/3 or 5) that project to the NAc core was observed (Wayman and Woodward, 2018b). Additionally, decreased intrinsic excitability was observed in the subset of layer 5/6 infralimbic neurons that project to the nucleus accumbens shell (Wayman and Woodward, 2018b). A subsequent study quantified the unique characteristics of Toluene-induced adaptations in excitability in PrL and infralimbic projection neurons and demonstrated that chemogenetic activation of accumbens projecting infralimbic cortex neurons prevents Toluene-induced conditioned place preference (Wayman and Woodward, 2018a). Taken together, these studies support the conclusion that hypoactivity in infralimbic to nucleus accumbens shell neurons promotes Toluene reward-associated behaviors. Finally, such a dichotomy is clearly drug-dependent as cue-induced heroin seeking (Rogers et al., 2008), morphine-induced conditioned place preference (Hearing et al., 2016), and cue-induced methamphetamine seeking (Kearns et al., 2022) all require activity in either the infralimbic cortex and/or its specific projection to the nucleus accumbens shell.

## Identification and Characterization of NAc<sup>PrL</sup> Neurons

Recent advances in AAV1-mediated transsynaptic transduction allow for the manipulation of neurons by virtue of their inputs (Zingg et al., 2017, 2020). Importantly, transsynaptic transgene expression is highly dependent on the number of active connections made between the upstream and downstream neuron (Zingg et al., 2017). Consistent with this property of AAV1 transsynaptic transduction, we found that 100% of virally transduced NAc<sup>PrL</sup> neurons responded when optically stimulating PrL terminals expressing DIO-hChR2, yet 58% of non-transduced cells either did not respond (33%) or showed a negligible response ( $\leq 10$  pA, 25%), and EPSC amplitude was significantly greater in NAc<sup>PrL</sup> neurons when compared to neighboring unlabeled cells. We observed that NAc<sup>PrL</sup> neurons represent  $\sim 10\%$  of total NeuN<sup>+</sup> neurons in the NAc core, the majority of which were MSNs. While this estimate is likely conservative given that this relies upon 100% transduction in the PrL, 1:1 transsynaptic transfer and 100% transduction in the NAc core, our data do support the existence of a subpopulation of NAc core neurons receiving the high density, functionally relevant PrL input.

## NAc<sup>PrL</sup> Neurons Are Required for Cue-Induced Reinstatement of Cocaine, but Not Sucrose, Seeking

The NAc core is a critical region mediating cue-induced seeking for all drugs of abuse (Kalivas and Volkow, 2011; Roberts-Wolfe and Kalivas, 2015; Spencer et al., 2018), whereby drug-induced cellular adaptations distinct from those induced by natural rewards set the stage for relapse vulnerability. Given the importance of the corticostriatal pathway in drug seeking (Figure 1) and the heterogeneity of PrL input density and

functional innervation of NAc core neurons (O'Donnell and Grace, 1995; Finch, 1996), we used AAV1 vectors to isolate and manipulate the NAc core MSNs most heavily innervated by the PrL cortex. We found that chemogenetic inhibition of NAc<sup>PrL</sup> neurons suppressed cue-induced cocaine, but not sucrose, seeking. One limitation of our approach is that NAc<sup>PrL</sup> neurons were transduced by virtue of their input from the PrL and not by virtue of their input *and* cell type. This is important given that we observed NAc<sup>PrL</sup> neurons constitute a mix of D1 and D2-expressing MSNs as well as interneurons. We suspect that chemogenetic inhibition of D1-NAc<sup>PrL</sup> and D2-NAc<sup>PrL</sup> neurons would have dichotomous effects on cued seeking, consistent with previous reports (Lobo et al., 2010; Heinsbroek et al., 2017). Our AAV1-derived estimates indicate that only 20% of total D2-MSNs receive dense PrL input, with NAc<sup>PrL</sup> neurons being approximately 50% D2-MSNs and by estimation 36% D1-MSNs. While just 7% of NAc<sup>PrL</sup> neurons were PV interneurons, 60% of total PV interneurons were labeled with our AAV1 transsynaptic vector, indicating that a large portion of total PV interneurons receive a functionally relevant PrL cortical input. As such, future experimentation will need to address whether chemogenetic inhibition of the population of PrL input receiving PV interneurons is necessary to suppress cue-induced reinstatement. Indeed, suppressing PV interneuron activity in the NAc reduces amphetamine sensitization in mice (Wang et al., 2018) and BLA-mediated activation of nucleus accumbens shell interneurons enhances acquisition of cocaine self-administration through interneuron-mediated inhibition of MSNs (Yu et al., 2017). A recent study also demonstrates that activation of NAc core PV interneurons in the NAc core produces conditioned place preference and reduces LiCl-induced conditioned place aversion (Chen et al., 2019). The authors find increased activation of D1 MSNs following optogenetic stimulation of NAc core PV interneurons and speculate that activation of PV interneurons in the NAc core promotes conditioned place preference through preferential targeting of MSNs in the indirect pathway or through polysynaptic disinhibition of direct pathway MSNs (Chen et al., 2019). Overall, the interaction between NAc<sup>PrL</sup> subtypes in regulating cocaine-seeking behavior is undoubtedly complex, and future studies will need to be performed to delineate the involvement of each specific subtype.

Regardless of the cell types involved, activity in NAc<sup>PrL</sup> neurons appears to be critical for overall NAc core activation during cocaine seeking given that chemogenetic inhibition of NAc<sup>PrL</sup> neurons led to an overall suppression of Fos<sup>+</sup> neurons in the NAc core. Consistent with recent reports (Bobadilla et al., 2020), we observed that overall levels of Fos induction in the NAc core per  $\mu\text{m}^3$  were similar in cocaine and sucrose reinstating mCherry control animals. However, Fos induction was significantly higher in NAc<sup>PrL</sup> neurons in mCherry cocaine animals compared to mCherry sucrose. Further, the magnitude of Fos activation in NAc<sup>PrL</sup> neurons positively correlated with the amount of seeking in cocaine, but not sucrose, animals. Collectively, these data demonstrate that NAc<sup>PrL</sup> neuronal activity is necessary for cue-induced cocaine, but not sucrose, seeking. Given that inhibition of PrL<sup>NAc core</sup> neurons

during cocaine seeking normalized NAc<sub>core</sub> glutamate levels to that of sucrose seeking animals (Figure 1), we speculate that both potentiated PrL-dependent excitatory transmission in the NAc<sub>core</sub> combined with cellular adaptations in NAc<sub>core</sub><sup>PrL</sup> neurons following extinction from cocaine, but not sucrose, SA sets the stage for relapse vulnerability. Additionally, when comparing the results from Figures 1, 3, the binned lever pressing data during cocaine seeking were not identical (Figure 1E vs. 3G). However, it is important to note that we did observe parity across these two distinct viral manipulations at different neurons, with an overall reduction in cue-induced cocaine seeking observed when inhibiting either PrL neurons the project to the NAc<sub>core</sub> (Figure 1), or NAc<sub>core</sub> neurons that receive PrL input (Figure 3).

## NAc<sub>core</sub><sup>PrL</sup> Neurons and Astrocytes Undergo Morphological Plasticity During Cocaine Seeking

Cue-induced seeking for multiple drugs of abuse elicits time-dependent increases in synaptic strength within the NAc<sub>core</sub> MSNs, including increased AMPA/NMDA ratio and enlarged dendritic spine  $d_H$  (Gipson et al., 2014), the degree of which positively correlates with drug-seeking behavior (Gipson et al., 2013a). As a recent addition to established cue-induced neuronal structural plasticity, heroin seeking has been linked to increased astrocyte association with NAc<sub>core</sub> synapses. This cue-induced astrocytic structural plasticity limits drug seeking (i.e., promotes within-session extinction), likely by increasing glutamate clearance (Kruyer et al., 2019). However, previous studies did not provide evidence that increased astrocyte association occurred at relevant synapses. Our data are the first to demonstrate that NAc<sub>core</sub><sup>PrL</sup> MSNs undergo increased dendritic spine  $d_H$  during the peak of reinstatement, as well as increased association of perisynaptic astrocyte processes with the most potentiated spines on NAc<sub>core</sub><sup>PrL</sup> neurons, an effect that was not observed 24 h following cocaine SA. These data suggest that cue-induced motility of astroglial processes and increased interaction with structurally potentiated synapses at NAc<sub>core</sub><sup>PrL</sup> MSNs serves to limit glutamate spillover during cocaine seeking.

## REFERENCES

- Augur, I. F., Wyckoff, A. R., Aston-Jones, G., Kalivas, P. W., and Peters, J. (2016). Chemogenetic activation of an extinction neural circuit reduces cue-induced reinstatement of cocaine seeking. *J. Neurosci.* 36, 10174–10180. doi: 10.1523/JNEUROSCI.0773-16.2016
- Bernardinelli, Y., Muller, D., and Nikonenko, I. (2014). Astrocyte-synapse structural plasticity. *Neural Plast.* 2014:232105.
- Bobadilla, A. C., Dereschewitz, E., Vaccaro, L., Heinsbroek, J. A., Scofield, M. D., and Kalivas, P. W. (2020). Cocaine and sucrose rewards recruit different seeking ensembles in the nucleus accumbens core. *Mol. Psychiatry* 25, 3150–3163. doi: 10.1038/s41380-020-00888-z
- Caballero, J. P., Scarpa, G. B., Remage-Healey, L., and Moorman, D. E. (2019). Differential effects of dorsal and ventral medial prefrontal cortex inactivation during natural reward seeking, extinction, and cue-induced reinstatement. *eNeuro* 6:ENEURO.296-ENEURO.219.

## DATA AVAILABILITY STATEMENT

The raw data supporting the conclusions of this article will be made available by the authors, without undue reservation.

## ETHICS STATEMENT

The animal study was reviewed and approved by the Institutional Committee for the Care and Use of Animals.

## AUTHOR CONTRIBUTIONS

BS performed all of the electrochemical studies, aided by MS. BS and SB performed the majority of the surgery, data analyses, and manuscript preparation. BS performed all of the microscopy with the analyses done by BS and MS. KV and LG performed the electrophysiological experimentation and data analyses. AB and AW performed the catheter surgery. AB, AW, and DD performed the rodent behavior. RK and DD performed the histological verification and mapping analyses. JO, CC, and MS aided in verification of data analyses and manuscript preparation. All authors contributed to the article and approved the submitted version.

## FUNDING

This work was funded by DA054154 (MS), DA050427 (BS), DA051650 (JO), DA032708 (CC), DA047845 (SB), the MUSC College of Medicine Enhancement of Team Science (COMETS) program (MS and JO), and NIDA Center on Cocaine and Opioid Addiction, DA046373 (CC and MS).

## SUPPLEMENTARY MATERIAL

The Supplementary Material for this article can be found online at: <https://www.frontiersin.org/articles/10.3389/fncel.2022.844243/full#supplementary-material>

- Carelli, R. M. (2002). Nucleus accumbens cell firing during goal-directed behaviors for cocaine vs. 'natural' reinforcement. *Physiol. Behav.* 76, 379–387. doi: 10.1016/s0031-9384(02)00760-6
- Chen, X., Liu, Z., Ma, C., Ma, L., and Liu, X. (2019). Parvalbumin interneurons determine emotional valence through modulating accumbal output pathways. *Front. Behav. Neurosci.* 13:110. doi: 10.3389/fnbeh.2019.00110
- Childress, A. R., Mozley, P. D., McElgin, W., Fitzgerald, J., Reivich, M., and O'Brien, C. P. (1999). Limbic activation during cue-induced cocaine craving. *Am. J. Psychiatry* 156, 11–18. doi: 10.1176/ajp.156.1.11
- Corkrum, M., Covelo, A., Lines, J., Bellocchio, L., Pisansky, M., Loke, K., et al. (2020). Dopamine-evoked synaptic regulation in the nucleus accumbens requires astrocyte activity. *Neuron* 105, 1036.e5–1047.e5. doi: 10.1016/j.neuron.2019.12.026
- Dallerac, G., Zapata, J., and Rouach, N. (2018). Versatile control of synaptic circuits by astrocytes: where, when and how? *Nat. Rev. Neurosci.* 19, 729–743. doi: 10.1038/s41583-018-0080-6
- Dumitriu, D., Laplant, Q., Grossman, Y. S., Dias, C., Janssen, W. G., Russo, S. J., et al. (2012). Subregional, dendritic compartment, and spine

- subtype specificity in cocaine regulation of dendritic spines in the nucleus accumbens. *J. Neurosci.* 32, 6957–6966. doi: 10.1523/JNEUROSCI.5718-11.2012
- Durkee, C. A., and Araque, A. (2019). Diversity and specificity of astrocyte-neuron communication. *Neuroscience* 396, 73–78. doi: 10.1016/j.neuroscience.2018.11.010
- Farrell, M. R., Schoch, H., and Mahler, S. V. (2018). Modeling cocaine relapse in rodents: Behavioral considerations and circuit mechanisms. *Prog. Neuropsychopharmacol. Biol. Psychiatry* 87, 33–47. doi: 10.1016/j.pnpbp.2018.01.002
- Finch, D. M. (1996). Neurophysiology of converging synaptic inputs from the rat prefrontal cortex, amygdala, midline thalamus, and hippocampal formation onto single neurons of the caudate/putamen and nucleus accumbens. *Hippocampus* 6, 495–512. doi: 10.1002/(SICI)1098-1063(1996)6:6<495::AID-HIPO3>3.0.CO;2-I
- Giannotti, G., Barry, S. M., Siemsen, B. M., Peters, J., and McGinty, J. F. (2018). Divergent prelimbic cortical pathways interact with bdnf to regulate cocaine-seeking. *J. Neurosci.* 38, 8956–8966. doi: 10.1523/JNEUROSCI.1332-18.2018
- Gipson, C. D., Kupchik, Y. M., and Kalivas, P. W. (2014). Rapid, transient synaptic plasticity in addiction. *Neuropharmacology* 76(Pt B), 276–286. doi: 10.1016/j.neuropharm.2013.04.032
- Gipson, C. D., Kupchik, Y. M., Shen, H., Reissner, K. J., Thomas, C. A., and Kalivas, P. W. (2013a). Relapse induced by cues predicting cocaine depends on rapid, transient synaptic potentiation. *Neuron* 77, 867–872. doi: 10.1016/j.neuron.2013.01.005
- Gipson, C. D., Reissner, K. J., Kupchik, Y. M., Smith, A. C., Stankeviciute, N., Hensley-Simon, M. E., et al. (2013b). Reinstatement of nicotine seeking is mediated by glutamatergic plasticity. *Proc. Natl. Acad. Sci. U.S.A.* 110, 9124–9129. doi: 10.1073/pnas.1220591110
- Girault, J. A. (2012). Integrating neurotransmission in striatal medium spiny neurons. *Adv. Exp. Med. Biol.* 970, 407–429. doi: 10.1007/978-3-7091-0932-8\_18
- Gordleeva, S. Y., Ermolaeva, A. V., Kastalskiy, I. A., and Kazantsev, V. B. (2019). Astrocyte as spatiotemporal integrating detector of neuronal activity. *Front. Physiol.* 10:294. doi: 10.3389/fphys.2019.00294
- Hearing, M. C., Jedynak, J., Ebner, S. R., Ingebreton, A., Asp, A. J., Fischer, R. A., et al. (2016). Reversal of morphine-induced cell-type-specific synaptic plasticity in the nucleus accumbens shell blocks reinstatement. *Proc. Natl. Acad. Sci. U.S.A.* 113, 757–762. doi: 10.1073/pnas.1519248113
- Heinsbroek, J. A., Neuhofer, D. N., Griffin, W. C. III, Siegel, G. S., Bobadilla, A. C., Kupchik, Y. M., et al. (2017). Loss of plasticity in the d2-accumbens pallidum pathway promotes cocaine seeking. *J. Neurosci.* 37, 757–767. doi: 10.1523/JNEUROSCI.2659-16.2016
- James, M. H., McGlinchey, E. M., Vattikonda, A., Mahler, S. V., and Aston-Jones, G. (2018). Cued reinstatement of cocaine but not sucrose seeking is dependent on dopamine signaling in prelimbic cortex and is associated with recruitment of prelimbic neurons that project to contralateral nucleus accumbens core. *Int. J. Neuropsychopharmacol.* 21, 89–94. doi: 10.1093/ijnp/pyx107
- Kalivas, P. W. (2008). Addiction as a pathology in prefrontal cortical regulation of corticostriatal habit circuitry. *Neurotox Res.* 14, 185–189. doi: 10.1007/BF03033809
- Kalivas, P. W. (2009). The glutamate homeostasis hypothesis of addiction. *Nat. Rev. Neurosci.* 10, 561–572. doi: 10.1038/nrn2515
- Kalivas, P. W., and O'Brien, C. (2008). Drug addiction as a pathology of staged neuroplasticity. *Neuropsychopharmacology* 33, 166–180. doi: 10.1038/sj.npp.1301564
- Kalivas, P. W., Volkow, N., and Seamans, J. (2005). Unmanageable motivation in addiction: a pathology in prefrontal-accumbens glutamate transmission. *Neuron* 45, 647–650. doi: 10.1016/j.neuron.2005.02.005
- Kalivas, P. W., and Volkow, N. D. (2011). New medications for drug addiction hiding in glutamatergic neuroplasticity. *Mol. Psychiatry* 16, 974–986. doi: 10.1038/mp.2011.46
- Kearns, A. M., Siemsen, B. M., Hopkins, J. L., Weber, R. A., Scofield, M. D., Peters, J., et al. (2022). Chemogenetic inhibition of corticostriatal circuits reduces cued reinstatement of methamphetamine seeking. *Addict. Biol.* 27:e13097. doi: 10.1111/adb.13097
- Keaveney, M. K., Rahsepar, B., Tseng, H. A., Fernandez, F. R., Mount, R. A., Ta, T., et al. (2020). CaMKIIalpha-positive interneurons identified via a microRNA-based viral gene targeting strategy. *J. Neurosci.* 40, 9576–9588. doi: 10.1523/JNEUROSCI.2570-19.2020
- Klug, J. R., Mathur, B. N., Kash, T. L., Wang, H. D., Matthews, R. T., Robison, A. J., et al. (2012). Genetic inhibition of CaMKII in dorsal striatal medium spiny neurons reduces functional excitatory synapses and enhances intrinsic excitability. *PLoS One* 7:e45323. doi: 10.1371/journal.pone.0045323
- Kosten, T. R., Scanley, B. E., Tucker, K. A., Oliveto, A., Prince, C., Sinha, R., et al. (2006). Cue-induced brain activity changes and relapse in cocaine-dependent patients. *Neuropsychopharmacology* 31, 644–650. doi: 10.1038/sj.npp.1300851
- Krueyer, A., Scofield, M. D., Wood, D., Reissner, K. J., and Kalivas, P. W. (2019). Heroin cue-evoked astrocytic structural plasticity at nucleus accumbens synapses inhibits heroin seeking. *Biol. Psychiatry* 86, 811–819. doi: 10.1016/j.biopsych.2019.06.026
- Lee, A. T., Vogt, D., Rubenstein, J. L., and Sohal, V. S. (2014). A class of GABAergic neurons in the prefrontal cortex sends long-range projections to the nucleus accumbens and elicits acute avoidance behavior. *J. Neurosci.* 34, 11519–11525. doi: 10.1523/JNEUROSCI.1157-14.2014
- Lobo, M. K., Covington, H. E. III, Chaudhury, D., Friedman, A. K., Sun, H., Dames-Werno, D., et al. (2010). Cell type-specific loss of BDNF signaling mimics optogenetic control of cocaine reward. *Science* 330, 385–390. doi: 10.1126/science.1188472
- Lu, X. Y., Ghasemzadeh, M. B., and Kalivas, P. W. (1998). Expression of D1 receptor, D2 receptor, substance P and enkephalin messenger RNAs in the neurons projecting from the nucleus accumbens. *Neuroscience* 82, 767–780. doi: 10.1016/s0306-4522(97)00327-8
- McGlinchey, E. M., James, M. H., Mahler, S. V., Pantazis, C., and Aston-Jones, G. (2016). Prelimbic to accumbens core pathway is recruited in a dopamine-dependent manner to drive cued reinstatement of cocaine seeking. *J. Neurosci.* 36, 8700–8711. doi: 10.1523/JNEUROSCI.1291-15.2016
- McLaughlin, J., and See, R. E. (2003). Selective inactivation of the dorsomedial prefrontal cortex and the basolateral amygdala attenuates conditioned-cue reinstatement of extinguished cocaine-seeking behavior in rats. *Psychopharmacology* 168, 57–65. doi: 10.1007/s00213-002-1196-x
- Moran, M. M., McFarland, K., Melendez, R. I., Kalivas, P. W., and Seamans, J. K. (2005). Cystine/glutamate exchange regulates metabotropic glutamate receptor presynaptic inhibition of excitatory transmission and vulnerability to cocaine seeking. *J. Neurosci.* 25, 6389–6393. doi: 10.1523/JNEUROSCI.1007-05.2005
- O'Donnell, P., and Grace, A. A. (1995). Synaptic interactions among excitatory afferents to nucleus accumbens neurons: hippocampal gating of prefrontal cortical input. *J. Neurosci.* 15, 3622–3639. doi: 10.1523/JNEUROSCI.15-05-03622.1995
- Oh, J. Y., Han, J. H., Lee, H., Han, Y. E., Rah, J. C., and Park, H. (2020). Labeling dual presynaptic inputs using cFork anterograde tracing system. *Exp. Neurobiol.* 29, 219–229. doi: 10.5607/en20006
- Otis, J. M., Zhu, M., Nambodiri, V. M. K., Cook, C. A., Kosyk, O., Matan, A. M., et al. (2019). Paraventricular thalamus projection neurons integrate cortical and hypothalamic signals for cue-reward processing. *Neuron* 103, 423.e4–431.e4. doi: 10.1016/j.neuron.2019.05.018
- Peters, J., LaLumiere, R. T., and Kalivas, P. W. (2008). Infralimbic prefrontal cortex is responsible for inhibiting cocaine seeking in extinguished rats. *J. Neurosci.* 28, 6046–6053. doi: 10.1523/JNEUROSCI.1045-08.2008
- Quiroz, C., Orru, M., Rea, W., Ciudad-Roberts, A., Yepes, G., Britt, J. P., et al. (2016). Local control of extracellular dopamine levels in the medial nucleus accumbens by a glutamatergic projection from the infralimbic cortex. *J. Neurosci.* 36, 851–859. doi: 10.1523/JNEUROSCI.2850-15.2016
- Richard, J. M., and Berridge, K. C. (2013). Prefrontal cortex modulates desire and dread generated by nucleus accumbens glutamate disruption. *Biol. Psychiatry* 73, 360–370. doi: 10.1016/j.biopsych.2012.08.009
- Roberts-Wolfe, D. J., and Kalivas, P. W. (2015). Glutamate transporter glt-1 as a therapeutic target for substance use disorders. *CNS Neurol. Disord. Drug Targets* 14, 745–756. doi: 10.2174/1871527314666150529144655
- Rogers, J. L., Ghee, S., and See, R. E. (2008). The neural circuitry underlying reinstatement of heroin-seeking behavior in an animal model of relapse. *Neuroscience* 151, 579–588. doi: 10.1016/j.neuroscience.2007.10.012
- Scofield, M. D., Heinsbroek, J. A., Gipson, C. D., Kupchik, Y. M., Spencer, S., Smith, A. C., et al. (2016a). The nucleus accumbens: mechanisms of addiction across

- drug classes reflect the importance of glutamate homeostasis. *Pharmacol. Rev.* 68, 816–871. doi: 10.1124/pr.116.012484
- Scofield, M. D., Li, H., Siemsen, B. M., Healey, K. L., Tran, P. K., Woronoff, N., et al. (2016b). Cocaine self-administration and extinction leads to reduced glial fibrillary acidic protein expression and morphometric features of astrocytes in the nucleus accumbens core. *Biol. Psychiatry* 80, 207–215. doi: 10.1016/j.biopsych.2015.12.022
- Shen, H., Moussawi, K., Zhou, W., Toda, S., and Kalivas, P. W. (2011). Heroin relapse requires long-term potentiation-like plasticity mediated by NMDA2b-containing receptors. *Proc. Natl. Acad. Sci. U.S.A.* 108, 19407–19412. doi: 10.1073/pnas.1112052108
- Siemsen, B. M., Giannotti, G., McFaddin, J. A., Scofield, M. D., and McGinty, J. F. (2018a). Biphasic effect of abstinence duration following cocaine self-administration on spine morphology and plasticity-related proteins in prelimbic cortical neurons projecting to the nucleus accumbens core. *Brain Struct. Funct.* 224, 741–758. doi: 10.1007/s00429-018-1805-z
- Siemsen, B. M., Lombroso, P. J., and McGinty, J. F. (2018b). Intra-prelimbic cortical inhibition of striatal-enriched tyrosine phosphatase suppresses cocaine seeking in rats. *Addict. Biol.* 23, 219–229. doi: 10.1111/adb.12504
- Siemsen, B. M., McFaddin, J. A., Haigh, K., Brock, A. G., Nan Leath, M., Hooker, K. N., et al. (2020). Amperometric measurements of cocaine cue and novel context-evoked glutamate and nitric oxide release in the nucleus accumbens core. *J. Neurochem.* 153, 599–616. doi: 10.1111/jnc.14952
- Siemsen, B. M., Reichel, C. M., Leong, K. C., Garcia-Keller, C., Gipson, C. D., Spencer, S., et al. (2019). Effects of methamphetamine self-administration and extinction on astrocyte structure and function in the nucleus accumbens core. *Neuroscience* 406, 528–541. doi: 10.1016/j.neuroscience.2019.03.040
- Smith, A. C. W., Scofield, M. D., Heinsbroek, J. A., Gipson, C. D., Neuhof, D., Roberts-Wolfe, D. J., et al. (2017). Accumbens nNOS interneurons regulate cocaine relapse. *J. Neurosci.* 37, 742–756. doi: 10.1523/JNEUROSCI.2673-16.2016
- Spencer, S., Neuhof, D., Chioma, V. C., Garcia-Keller, C., Schwartz, D. J., Allen, N., et al. (2018). A model of delta(9)-tetrahydrocannabinol self-administration and reinstatement that alters synaptic plasticity in nucleus accumbens. *Biol. Psychiatry* 84, 601–610. doi: 10.1016/j.biopsych.2018.04.016
- Stefanik, M. T., Kupchik, Y. M., and Kalivas, P. W. (2016). Optogenetic inhibition of cortical afferents in the nucleus accumbens simultaneously prevents cue-induced transient synaptic potentiation and cocaine-seeking behavior. *Brain Struct. Funct.* 221, 1681–1689. doi: 10.1007/s00429-015-0997-8
- Stefanik, M. T., Moussawi, K., Kupchik, Y. M., Smith, K. C., Miller, R. L., Huff, M. L., et al. (2013). Optogenetic inhibition of cocaine seeking in rats. *Addict. Biol.* 18, 50–53. doi: 10.1111/j.1369-1600.2012.00479.x
- Testen, A., Sepulveda-Orengo, M. T., Gaines, C. H., and Reissner, K. J. (2018). Region-specific reductions in morphometric properties and synaptic colocalization of astrocytes following cocaine self-administration and extinction. *Front. Cell Neurosci.* 12:246. doi: 10.3389/fncel.2018.00246
- Wang, X., Gallegos, D. A., Pogorelov, V. M., O'Hare, J. K., Calakos, N., Wetsel, W. C., et al. (2018). Parvalbumin interneurons of the mouse nucleus accumbens are required for amphetamine-induced locomotor sensitization and conditioned place preference. *Neuropsychopharmacology* 43, 953–963. doi: 10.1038/npp.2017.178
- Wayman, W. N., and Woodward, J. J. (2018a). Chemogenetic excitation of accumbens-projecting infralimbic cortical neurons blocks toluene-induced conditioned place preference. *J. Neurosci.* 38, 1462–1471. doi: 10.1523/JNEUROSCI.2503-17.2018
- Wayman, W. N., and Woodward, J. J. (2018b). Exposure to the abused inhalant toluene alters medial prefrontal cortex physiology. *Neuropsychopharmacology* 43, 912–924. doi: 10.1038/npp.2017.117
- Weiss, F., Paulus, M. P., Lorang, M. T., and Koob, G. F. (1992). Increases in extracellular dopamine in the nucleus accumbens by cocaine are inversely related to basal levels: effects of acute and repeated administration. *J. Neurosci.* 12, 4372–4380. doi: 10.1523/JNEUROSCI.12-11-04372.1992
- Yu, J., Yan, Y., Li, K. L., Wang, Y., Huang, Y. H., Urban, N. N., et al. (2017). Nucleus accumbens feedforward inhibition circuit promotes cocaine self-administration. *Proc. Natl. Acad. Sci. U.S.A.* 114, E8750–E8759. doi: 10.1073/pnas.1707822114
- Zingg, B., Chou, X. L., Zhang, Z. G., Mesik, L., Liang, F., Tao, H. W., et al. (2017). AAV-mediated anterograde transsynaptic tagging: mapping corticocollicular input-defined neural pathways for defense behaviors. *Neuron* 93, 33–47. doi: 10.1016/j.neuron.2016.11.045
- Zingg, B., Peng, B., Huang, J., Tao, H. W., and Zhang, L. I. (2020). Synaptic specificity and application of anterograde transsynaptic AAV for probing neural circuitry. *J. Neurosci.* 40, 3250–3267. doi: 10.1523/JNEUROSCI.2158-19.2020

**Conflict of Interest:** The authors declare that the research was conducted in the absence of any commercial or financial relationships that could be construed as a potential conflict of interest.

**Publisher's Note:** All claims expressed in this article are solely those of the authors and do not necessarily represent those of their affiliated organizations, or those of the publisher, the editors and the reviewers. Any product that may be evaluated in this article, or claim that may be made by its manufacturer, is not guaranteed or endorsed by the publisher.

Copyright © 2022 Siemsen, Barry, Vollmer, Green, Brock, Westphal, King, DeVries, Otis, Cowan and Scofield. This is an open-access article distributed under the terms of the Creative Commons Attribution License (CC BY). The use, distribution or reproduction in other forums is permitted, provided the original author(s) and the copyright owner(s) are credited and that the original publication in this journal is cited, in accordance with accepted academic practice. No use, distribution or reproduction is permitted which does not comply with these terms.